

Policy iteration using Q-functions: Linear dynamics with multiplicative noise.[★]

Peter Coppens^{*} Panagiotis Patrinos^{*}

^{*} *Department of Electrical Engineering (ESAT-STADIUS), KU
Leuven, Kasteelpark Arenberg 10, 3001 Leuven, Belgium. Email:
peter.coppens@kuleuven.be, panos.patrinis@kuleuven.be*

Abstract: This paper presents a novel model-free and fully data-driven policy iteration scheme for quadratic regulation of linear dynamics with state- and input-multiplicative noise. The implementation is similar to the *least-squares temporal difference* scheme for Markov decision processes, estimating Q-functions by solving a least-squares problem with instrumental variables. The scheme is compared with a model-based system identification scheme and natural policy gradient through numerical experiments.

Keywords: Data-driven optimal control, Stochastic optimal control problems, Reinforcement learning, Linear systems, Parameter-varying systems.

1. INTRODUCTION

The success story of AlphaZero in Silver et al. (2017) and similar reinforcement learning strategies in a variety of applications has reinvigorated the interest of the control community in learning schemes. Many of these fall under the general framework of dynamic programming, policy iteration, etc. (see Bertsekas (2022a,b) for a good overview). Hence understanding the performance of such schemes in simple settings can generalize to more complex problems. One setting under investigation has been *Linear Quadratic Regulation (LQR)*. For example Recht (2019); Mania et al. (2019); Dean et al. (2019) consider *model-based* approaches where system identification is performed separately from control synthesis. In Bradtke et al. (1994); Lewis and Vrabie (2009); Bu et al. (2019) meanwhile *model-free* approaches – more akin to usual reinforcement learning – like policy iteration and policy gradient – were investigated.

A setting with similar potential is quadratic regulation of linear dynamics with multiplicative noise (Wonham, 1967). Here analytical solutions are still available, yet several challenges absent from classical LQR present themselves. For example, the optimal controller depends on the first and second moment of the noise – unlike in LQR with additive noise – and the separation principle does not hold. Moreover, as we will see, data-driven policy evaluation is not possible through normal least-squares as in (Bradtke et al., 1994) and instead requires instrumental variables as is the case with Markov decision processes (Bradtke, 1996). Multiplicative noise also arises naturally in aerospace and

vehicle control applications (Damm, 2004, §1.9), biological applications (Todorov, 2005; Mohler et al., 1980) and communication channels (Wang and Balakrishnan, 2002) among others. Finally, the inclusion of multiplicative noise also induces robustness against parametric uncertainty (Coppens and Patrinos, 2022; Gravell et al., 2020), which is especially helpful in data-driven applications.

For multiplicative noise the *model-based* setting has already been investigated in Coppens et al. (2020); Coppens and Patrinos (2020, 2022); Xing et al. (2021). Policy gradient was investigated in Gravell et al. (2021) and policy iteration in Wang et al. (2018); Gravell et al. (2022). The last two results however assumed the possibility of exact policy evaluation, which is only possible for known dynamics.

In this work we provide a data-driven scheme for policy iteration applied to linear dynamics with multiplicative noise. The approximate policy evaluation step is based on Q-functions as in Bradtke et al. (1994) with the *instrumental variables* used for *least squares temporal difference (LSTD)* learning in Bradtke (1996). Our scheme can both operate in an *off-policy* setting – where data-generation happens with some fixed, pre-determined policy – and in an *on-policy* setting, where the last policy iterate is applied to the dynamics with some additive noise to enable exploration.

The remainder of this paper begins with a problem definition in §2. Next, in §3 a novel approximate policy evaluation scheme using Q-functions is derived, which is integrated in a policy iteration scheme in §4. We also review an existing model-based scheme (Coppens and Patrinos, 2022) and a policy gradient scheme (Gravell et al., 2021). In §5 we then compare the performance and applicability of these three data-driven control schemes. In §6 we then conclude the paper and suggest further work.

Notation: Let \mathbb{R} denote the reals and \mathbb{N} the naturals. For $Z \in \mathbb{R}^{m \times n}$ let Z^\top denote the transpose and let

[★] This work is supported by: the Research Foundation Flanders (FWO) PhD grant 11E5520N and research projects G081222N, G033822N, G0A0920N; European Union’s Horizon 2020 research and innovation programme under the Marie Skłodowska-Curie grant agreement No. 953348; Research Council KU Leuven C1 project No. C14/18/068; Fonds de la Recherche Scientifique - FNRS and the Fonds Wetenschappelijk Onderzoek - Vlaanderen under EOS project no 30468160 (SeLMA).

$\|Z\|_2$ ($\|Z\|_F$) be the spectral (Frobenius) norm. When $Z \in \mathbb{R}^{n \times n}$ let $\lambda(Z) = (\lambda_1, \dots, \lambda_m)$ denote the vector of eigenvalues in descending order of modulus and $\rho(Z) = |\lambda_1(Z)|$ the spectral radius. For a vector $x \in \mathbb{R}^d$ let $\|x\|_2$ denote the Euclidean norm. Let $\mathbb{E}[\cdot]$ denote the expectation.

We denote by \mathbb{S}^d the set of symmetric d by d matrices and by \mathbb{S}_{++}^d (\mathbb{S}_+^d) the positive (semi)definite matrices. Moreover $X - Y \succ (\succeq) 0$ denotes $X - Y \in \mathbb{S}_{++}^d$ (\mathbb{S}_+^d). Let $\mathfrak{s}_d = (d+1)d/2$ denote the degrees of freedom of elements of \mathbb{S}^d and $\text{vec}_s(X) \in \mathbb{R}^{\mathfrak{s}_d}$ denotes the symmetrized vectorization (Coppens and Patrinos, 2022, §III.A) such that $\text{vec}_s(X)^\top \text{vec}_s(Y) = \text{Tr}[XY]$ and $\|\text{vec}_s(X)\|_2 = \|X\|_F$, with $\text{unvec}_s: \mathbb{R}^{\mathfrak{s}_d} \rightarrow \mathbb{R}^d$ its inverse.

For matrices of conformable size X, Y we use $[X, Y]$ for horizontal concatenation, let (x, y) denote vertical concatenation between (column) vectors and let $I_d \in \mathbb{R}^{d \times d}$ be the identity. Elements of matrices $X \in \mathbb{R}^{m \times n}$ (and vectors $x \in \mathbb{R}^d$) are indexed using X_{ij} (x_i) for $i \in \{1, \dots, m\}$, $j \in \{1, \dots, n\}$ ($i \in \{1, \dots, d\}$). For a matrix-valued operator $\mathcal{E}: \mathbb{S}^n \rightarrow \mathbb{S}^m$ we similarly write $\mathcal{E}_{ij}: \mathbb{S}^n \rightarrow \mathbb{R}$. Moreover $\mathcal{E}^*: \mathbb{S}^m \rightarrow \mathbb{S}^n$ is the adjoint, such that $\text{Tr}[P\mathcal{E}(X)] = \text{Tr}[\mathcal{E}^*(P)X]$ for all $X \in \mathbb{S}^n$ and $P \in \mathbb{S}^m$.

2. PROBLEM SETUP

Consider linear systems with input- and state-multiplicative noise, given for all $t \in \mathbb{N}$ as:

$$x_{t+1} = \left(\sum_{\ell=1}^{n_w} A_i w_{t,\ell} \right) x_t + \left(\sum_{\ell=1}^{n_w} B_i w_{t,\ell} \right) u_t, \quad (1)$$

with $x_t \in \mathbb{R}^{n_x}$ the state, $u_t \in \mathbb{R}^{n_u}$ the input and $w_t \in \mathbb{R}^{n_w}$ the i.i.d. random disturbance.

The goal is to solve

$$\underset{u_0, u_1, \dots}{\text{minimize}} \quad \mathbb{E} \left[\sum_{t=0}^{\infty} x_t^\top Q x_t + u_t^\top R u_t \right], \quad (2)$$

subject to (1) with $Q \succ 0$ and $R \succ 0$ when only given access to trajectories $\{(x_t, u_t)\}_{t=0}^T$ of (1). The way in which these trajectories are generated (e.g. what policy to use) will be discussed in §4.1.

Often it is more convenient to consider the evolution of the second moments $X_t := \mathbb{E}[x_t x_t^\top]$, $Z_t := \mathbb{E}[z_t z_t^\top]$, with $z_t = (x_t, u_t)$ the augmented state, when solving (2). These follow the dynamics

$$X_{t+1} = \mathcal{E}(Z_t) := \sum_{i,j=1}^{n_w} W_{ij} [A_i, B_i] Z_t [A_j, B_j]^\top, \quad (3)$$

with $W := \mathbb{E}[w_t w_t^\top]$ – independent of t due to the i.i.d. assumption. The LQR problem (2) then becomes

$$J_\star(X_0) := \underset{Z_0, Z_1, \dots}{\text{minimize}} \quad \sum_{t=0}^{\infty} \text{Tr}[H Z_t], \quad (4)$$

subject to $Z_t \succeq 0$ and (3) starting from X_0 and where $H = \text{diag}(Q, R) \succ 0$. We refer to $J(X_0)$ as the value function. Equivalence of (2) and (4) was shown in (Coppens and Patrinos, 2022, Prop. IV.6), where the properties of \mathcal{E} – a *completely positive (CP) operator* – were studied.

Since we will often deal with partitionings of matrices like $Z \in \mathbb{S}^{n_z}$ we introduce the subscripts:

$$Z = \begin{bmatrix} Z_{xx} & Z_{ux}^\top \\ Z_{ux} & Z_{uu} \end{bmatrix}, \quad (5)$$

where $Z_{xx} \in \mathbb{S}^{n_x}$ and analogously for the other terms.

3. APPROXIMATE POLICY EVALUATION

It is well known that the optimal policy solving (2) is linear (cf. (Coppens and Patrinos, 2022, Thm. IV.8)). In terms of moments such policies look like

$$Z_t = \pi(X_t) := [I, K^\top]^\top X_t [I, K^\top], \quad (6)$$

We will refer to K and π interchangeably as the policy.

As usual, to derive our policy iteration algorithm we need to consider the Bellman operator (Bertsekas, 2022a, §1.2):

$$(\mathcal{T}_\pi J)(X) = \text{Tr}[\pi(X)H] + J[\mathcal{E}(\pi(X))], \quad \forall X \succeq 0. \quad (7)$$

and $\mathcal{T}J := \min_\pi \mathcal{T}_\pi J$, operating on $J: \mathbb{S}^{n_x} \rightarrow \mathbb{R}$.

If the dynamics are stabilizable (i.e. there exists a mean-square stabilizing controller), then the optimal value of (4) is given as the fixed-point of \mathcal{T} . Moreover the optimal controller is then $\text{argmin}_\pi \mathcal{T}_\pi J_\star$ of (7) with $J_\star = \mathcal{T}J_\star$ (Coppens and Patrinos, 2022, Thm. IV.8).

In our case we know that the value function is linear in the second moment¹, i.e. $J(X) = \text{Tr}[XP]$ for some $P \succ 0$. Plugging in this parametrization and (6) and using the definition of the adjoint gives:

$$(\mathcal{T}J)(X) = \min_K \text{Tr}[X[I, K^\top](H + \mathcal{E}^*(P))[I, K^\top]^\top].$$

The minimizer, stated using the subscripts in (5), is given as $K_\star = -(R + \mathcal{E}_{uu}^*(P))^{-1} \mathcal{E}_{ux}^*(P)$. Now $J = \mathcal{T}J$ can be written in terms of P as

$$P = Q + \mathcal{E}_{xx}^*(P) - \mathcal{E}_{ux}^*(P)^\top (R + \mathcal{E}_{uu}^*(P))^{-1} \mathcal{E}_{ux}^*(P). \quad (8)$$

This generalized Riccati equation is derived in detail and solved using a SDP in (Coppens and Patrinos, 2022, Thm. IV.10).

We intend to find K_\star through *policy iteration*, which repeatedly updates π by finding a π_+ such that

$$\pi_+ = \underset{\pi'}{\text{argmin}} \mathcal{T}_{\pi'} J_\pi, \quad \text{with } J_\pi = \mathcal{T}_\pi J_\pi. \quad (9)$$

Finding J_π is called *policy evaluation* and requires solving a Lyapunov equation. Again using a parametrization $J_\pi(X) = \text{Tr}[P_\pi X]$, we write $J_\pi = \mathcal{T}_\pi J_\pi$ as:

$$\begin{aligned} \text{Tr}[X P_\pi] &= \text{Tr}[\pi(X)H] + \text{Tr}[P_\pi \mathcal{E}(\pi(X))] \\ &= \text{Tr}[X \pi^*(H + \mathcal{E}^*(P_\pi))], \end{aligned} \quad (10)$$

for all X , where we used the definition of the adjoint. Thus we recover the following Lyapunov equation²:

$$\begin{aligned} P_\pi &= \pi^*(H + \mathcal{E}^*(P_\pi)) \\ \Leftrightarrow P_\pi &= (I - \pi^*(\mathcal{E}^*))^{-1} (\pi^*(H)). \end{aligned} \quad (11)$$

Several schemes exist to solve such equations using data (cf. (Bertsekas, 2012, §6) and Bradtke (1996) for MDPs). However, even after finding J_π , computing the minimizer in (9) requires the dynamics. Hence we use Q-functions.

¹ It is thus quadratic in the state

² For a proof of invertibility when π is mean-square stabilizing see (Coppens and Patrinos, 2022, Prop. III.8).

3.1 Q-functions

A Q-function in this setting maps Z to some real number. We consider the Bellman operator on Q-functions:

$$(\mathcal{F}_\pi \mathcal{Q})(Z) = \text{Tr}[ZH] + \mathcal{Q}(\pi(\mathcal{E}(Z)))$$

and $\mathcal{F}\mathcal{Q} := \min_\pi \mathcal{F}_\pi \mathcal{Q}$. For some policy π we define \mathcal{Q}_π as

$$\mathcal{Q}_\pi(Z) := \text{Tr}[ZH] + J_\pi[\mathcal{E}(Z)], \quad (12)$$

where J_π solves $J_\pi = \mathcal{T}_\pi J_\pi$ (cf. (10)). We can show that this choice of \mathcal{Q}_π is a fixed-point of \mathcal{F}_π :

$$\begin{aligned} (\mathcal{F}_\pi \mathcal{Q}_\pi)(Z) &= \text{Tr}[ZH] + \text{Tr}[\pi(\mathcal{E}(Z))H] + J_\pi[\mathcal{E}(\pi(\mathcal{E}(Z)))] \\ &= \text{Tr}[ZH] + (\mathcal{T}_\pi J_\pi)[\mathcal{E}(Z)] \\ &= \text{Tr}[ZH] + J_\pi[\mathcal{E}(Z)] = \mathcal{Q}_\pi(Z), \end{aligned}$$

where we used the definition of \mathcal{T}_π for the second equality and $J_\pi = \mathcal{T}_\pi J_\pi$ for the third.

Given such a \mathcal{Q}_π we implement policy iteration as:

$$\pi_+(X) = \underset{\pi'}{\text{argmin}} \mathcal{Q}_\pi(\pi'(X)),$$

which is equivalent to $\pi_+ = \underset{\pi'}{\text{argmin}} \mathcal{F}_{\pi'} \mathcal{Q}_\pi$ (and thus (9)) yet requires no knowledge about the dynamics. Using a linear parametrization $\mathcal{Q}_\pi = \text{Tr}[\Theta_\pi Z]$ we get

$$K_+ = -(\Theta_\pi)_{uu}^{-1}(\Theta_\pi)_{ux}.$$

Comparing with K_* from the previous section further confirms that the optimal gain can be recovered by selecting the correct value for Θ_π .

3.2 Least-Squares

In our data-driven setting, solving (10) to perform the policy evaluation is challenging, since we need to evaluate \mathcal{E} . In Wang et al. (2018) it was assumed that it could be evaluated exactly, which requires knowing the true dynamics. Instead, similarly to Bradtke et al. (1994), we opt to estimate \mathcal{Q}_π directly from data. We begin by discussing constraints on the data and then derive a model equation used for a least-squares estimator.

We assume access to samples of subsequent moments $\{(Z_i, Z_{i+})\}_{i=1}^N$, where $Z_{i+} = \pi(X_{i+}) = \pi(\mathcal{E}_i(Z_i))$ with

$$\mathcal{E}_i(Z_i) := \sum_{j,\ell=1}^{n_w} (w_{i,j} w_{i,\ell}) [A_j, B_j] Z_i [A_\ell, B_\ell]^\top. \quad (13)$$

Such data can be generated by taking some z_i and evaluating x_{i+} with (1). Then let $Z_i = z_i z_i^\top$ and $Z_{i+} = \pi(x_{i+} x_{i+}^\top)$. We give a detailed data-generation procedure in §4.1.

We want to find \mathcal{Q}_π such that $\mathcal{Q}_\pi(Z) = (\mathcal{F}_\pi \mathcal{Q}_\pi)(Z)$ for all $Z \in \mathbb{S}_+^{n_z}$. To do so we sample $\mathcal{F}_\pi \mathcal{Q}_\pi$:

$$(\mathcal{F}_\pi^i \mathcal{Q}_\pi)(Z_i) := \text{Tr}[Z_i H] + \mathcal{Q}_\pi(Z_{i+}), \quad (14)$$

which we can use to construct a model equation:

$$\mathcal{Q}_\pi(Z_i) = (\mathcal{F}_\pi^i \mathcal{Q}_\pi)(Z_i) + ((\mathcal{F}_\pi \mathcal{Q}_\pi)(Z_i) - (\mathcal{F}_\pi^i \mathcal{Q}_\pi)(Z_i)).$$

Using the parametrization $\mathcal{Q}_\pi(Z) = \text{Tr}[\Theta_\pi Z]$ results in:

$$\begin{aligned} \text{Tr}[\Theta_\pi Z_i] &= \text{Tr}[Z_i H] + \text{Tr}[\Theta_\pi Z_{i+}] \\ &\quad + \text{Tr}[\Theta_\pi \pi(\mathcal{E}(Z_i) - \mathcal{E}_i(Z_i))], \end{aligned} \quad (15)$$

which is linear in the parameter Θ_π with zero-mean error. Note that (15) involves a *temporal differences* as in Bradtke (1996).

We reframe the model using the symmetric vectorization operator $\text{vec}_s: \mathbb{S}^n \mapsto \mathbb{R}^{\delta_n}$ with $\delta_n := n(n+1)/2$ (cf.

(Coppens and Patrinos, 2022, §III.A)), which satisfies $\text{Tr}[XY] = \text{vec}_s(X)^\top \text{vec}_s(Y)$. Its inverse is denoted as unvec_s . We rewrite (15) as:

$$b_i = (a_i + e_i)^\top \theta_\pi, \quad (16)$$

with $\theta_\pi = \text{vec}_s(\Theta_\pi)$, $b_i = \text{Tr}[H Z_i]$, $a_i = \text{vec}_s(Z_i - Z_{i+})$ and $e_i = \text{vec}_s(Z_{i+} - \pi(\mathcal{E}(Z_i)))$. This is known as the error-in-variables setting. The challenge is that both a_i and e_i linearly depend on $w_i w_i^\top$ through $Z_{i+} = \pi(\mathcal{E}_i(Z_i))$. Hence $\mathbb{E}[a_i e_i^\top] \neq 0$, which makes a classical least-squares estimate inconsistent.

This is the classical motivation for *instrumental variables* (IVs) (Young, 2011, §3.3). We use $g_i := \text{vec}_s(Z_i)$ as IVs similarly to Bradtke (1996). This choice is independent of the error e_i (i.e. $\mathbb{E}[g_i e_i^\top] = 0$), yet is correlated with $a_i + e_i$ as desired of an IV. Intuitively, g_i can be viewed as its best estimate without any additional information on the dynamics \mathcal{E} . We further motivate the choice by linking it to a projected Bellman equation in §A.

The estimate using the IVs is

$$\hat{\theta}_\pi = \left(\sum_{i=1}^N g_i a_i^\top \right)^{-1} \left(\sum_{i=1}^N g_i b_i \right).$$

Alternatively we can use the recursive algorithm:

$$\begin{aligned} \hat{\theta}_{\pi,i} &= \hat{\theta}_{\pi,i-1} + L_i [b_i - a_i^\top \hat{\theta}_{\pi,i-1}] \\ L_i &= S_{\pi,i-1} g_i / (1 + a_i^\top S_{\pi,i-1} g_i) \\ S_{\pi,i} &= S_{\pi,i-1} - (L_i a_i^\top) S_{\pi,i-1} \end{aligned} \quad (17)$$

for $i = 1, \dots, N$ and where the initialization $\hat{\theta}_{\pi,0} \in \mathbb{R}^{\delta_{n_z}}$ and $S_{\pi,0} \in \mathbb{R}^{\delta_{n_z} \times \delta_{n_z}}$ can be interpreted as an initial guess for θ_π and the confidence in that guess respectively.

4. LEARNING CONTROL SCHEMES

We provide an overview of learning control schemes for the dynamics (1). To enable consistent comparisons we first describe a general scheme for gathering data. Then we describe our new policy iteration algorithm. Next we briefly summarize the system identification procedure of Coppens and Patrinos (2022) and the policy gradient scheme of Gravell et al. (2021). Sample complexity guarantees are reported whenever they exist.

4.1 Data-generation

We describe the data generation process. To enable comparison of the presented algorithms we view them as all iteratively updating the policy, where M trajectories (or rollouts) of length T for a total of $N = MT$ new data points satisfying (13) are used each iteration. Specifically we simulate in parallel for $j = 1, \dots, M$ and $k = 0, \dots, T$:

$$x_{k+1}^j = \left(\sum_{\ell=1}^{n_w} A_\ell w_{k,\ell}^j \right) x_k^j + \left(\sum_{\ell=1}^{n_w} B_\ell w_{k,\ell}^j \right) u_k^j,$$

and let $z_k^j = (x_k^j, u_k^j)$ for

$$u_k^j = (K + U^j) x_k^j + \nu_k^j. \quad (18)$$

Here U^j and ν_k^j are uniformly distributed over $\{U: \|U\|_F = r_U\}$ and $\{\nu: \|\nu\|_2 \leq r_\nu\}$ respectively. The controller perturbation U^j is sampled at the start of a trajectory and ν_k^j at each time step. Moreover U^j is distributed over a

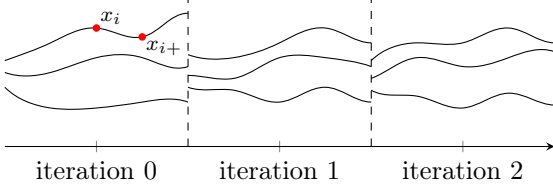


Figure 1. Rollouts used for data-generation.

sphere, instead of a ball, since in policy gradient, it is used to estimate the gradient of the infinite horizon cost through finite differences as explained in Alg. 2 later. We sample ν_k^j from a ball to avoid over-excitation of the system, while keeping the trajectories informative enough.

We depict the procedure in Fig. 1. Since only states and inputs are gathered, the functional form of the dynamics is not required. Only a simulator or experiments are required.

Each trajectory has to be initialized at the start of a new controller iteration. We can either continue trajectories from the previous iteration (henceforth referred to as *continuous mode*), or we sample $\{x_0^j\}_{j=1}^M$ uniformly from $\{x: \|x\|_2 \leq r_x\}$.

We estimate the moments X_k^j and Z_k^j for each (augmented) state vector by taking an outer product. When the specific trajectory does not affect the identification procedure (as in policy iteration and system identification) we write (Z_i, X_{i+}) to index the pairs (Z_k^j, X_{k+1}^j) , for k and j varying within their range. These pairs all satisfy (13).

4.2 Policy Iteration (PI)

Based on the discussion in the previous section we can now state the full approximate policy iteration algorithm. *Generate pair* refers to the rollouts described in the previous section.

Algorithm 1: Approximate policy iteration.

Data: Initial guess $\hat{\theta}_{\pi_0}$, number of samples N and confidence parameter β_0 .

Initialize $S_{\pi_0} = \beta_0 I$.

for $k = 1$ **to** ∞ **do**

$K_k = -\Theta_{uu}^{-1} \Theta_{ux}$, with $\Theta = \text{unvec}_s(\hat{\theta}_{\pi_{k-1}})$.

Let $\hat{\theta}_{\pi_k,0} = \hat{\theta}_{\pi_{k-1}}$ and $S_{\pi_k,0} = S_{\pi_{k-1}}$.

for $i = 1$ **to** N **do**

Generate pair (Z_i, X_{i+}) and let

$Z_{i+} = \pi_k(X_{i+})$.

Update $\hat{\theta}_{\pi_k,i}$, $S_{\pi_k,i}$ using (17).

end

Set $\hat{\theta}_{\pi_k} = \hat{\theta}_{\pi_k,N}$ and $S_{\pi_k} = S_{\pi_k,N}$.

end

Note how we use the confidence at the end of the previous policy iteration $S_{\pi_{k-1}}$ to initialize the next. This on a high-level corresponds to keeping a summary of the data from past policies and is contrasted by Bradtke et al. (1994), where $S_{\pi_k,0}$ in (17) is reset to $\beta_0 I$ at the start of each policy iteration. Our approach enables the scheme to keep improving its estimate of the Q-function as is confirmed in the numerical experiments. To theoretical back this

decision we provide an alternative interpretation as an Extended Kalman Filter (Bertsekas, 2016, §2.4.3) applied to a projected Bellman equation in §A

4.3 System Identification (SI)

The data generated for the policy iteration scheme in the previous section can also be used to identify the dynamics. We have the following model equation for $i = 1, \dots, N$:

$$X_{i+} = \mathcal{E}(Z_i) + (\mathcal{E}_i(Z_i) - \mathcal{E}(Z_i)),$$

with \mathcal{E}_i as in (13). The model equation is linear in the matrix representing the linear map \mathcal{E} and has a zero-mean error. Hence we can estimate \mathcal{E} using least-squares as in Coppens and Patrinos (2022). The resulting least-squares problem has $N\mathfrak{z}_{n_x}$ equations and $\mathfrak{z}_{n_z}\mathfrak{z}_{n_x}$ parameters describing the matrix of the linear map $\mathcal{E}: \mathbb{S}^{n_z} \rightarrow \mathbb{S}^{n_x}$. The advantage of this scheme is that prior knowledge about the dynamics, like the mode matrices A_i and B_i , can be included to reduce the problem complexity. In this case we estimate $\mathbb{E}[ww^\top]$ instead of \mathcal{E} . Given the dynamics, the optimal controller can be computed by solving a semi-definite program (Coppens and Patrinos, 2022, Thm. IV.10). In the experiments below we do this once per iteration, where the least-square estimate is updated recursively using (Bertsekas, 2016, Prop. 1.5.2, Eq. 1.118).

Theoretical guarantees are provided in (Coppens and Patrinos, 2022, Thm VI.4, Rem. VI.5), which states³ that for a sub-optimality ϵ the required number of samples is of order $1/\epsilon$.

4.4 Policy Gradient (PG)

We summarize the model-free policy gradient scheme described in Gravell et al. (2021). Given some η and initial guess K_0 we can compute the optimal controller directly via natural gradient descent:

$$K_{k+1} = K_k - \eta \nabla \widehat{J(K)} \Sigma_K, \quad (19)$$

where the gradient and $\Sigma_K := \sum_{t=0}^{\infty} X_t$ with X_t the closed-loop trajectory with gain K is computed in data-driven fashion using the following algorithm:

Algorithm 2: Gradient evaluation.

Data: Gain matrix K , number of rollouts M , rollout length T and exploration radius r_U .

Generate $\{Z_t^j\}$ for $j = 1, \dots, M$, $k = 1, \dots, T$ with policy (18) for $r_\nu = 0$, r_U and K as provided.

Let $\hat{J}_j = \sum_{t=0}^T \text{Tr}[Z_t^j H]$ and $\hat{\Sigma}^j = \sum_{t=0}^T (Z_t^j)_{xx}$.

return $\nabla \widehat{J(K)} = \sum_{j=1}^M \frac{n_x n_y}{M r^2} \hat{J}_j U_j$, $\hat{\Sigma}_K = \frac{1}{M} \sum_{j=1}^M \hat{\Sigma}^j$.

Note that this algorithm requires *on-policy* exploration. Moreover multiple rollouts should be generated to get a suitable estimate of \hat{J}_j in each iteration. So policy gradient restricts data-generation more than the other methods.

Theoretical guarantees for classical gradient (i.e. using $\Sigma_K = I$) are available in (Gravell et al., 2021, Thm. 5.1). Given some desired accuracy ϵ , one should select $M =$

³ The theoretical guarantees only hold for trajectories of length one or when only the final transition of each trajectory is used. The rate was verified empirically for more general settings.

$\mathcal{O}(1/\epsilon^2)$, $T = \mathcal{O}(1/\epsilon^2)$ and $r_U = \mathcal{O}(\epsilon)$ in the gradient evaluation step. The gradient descent scheme will then converge at a linear rate to some K such that the suboptimality is bounded by ϵ . Hence the total sample complexity is of order $1/\epsilon^4$. In later experiments we illustrate a case with $1/\epsilon$ sample complexity. The stated rates are however asymptotic and for classical gradient descent. So the observed gap could disappear for larger sample counts or is caused by natural gradient descent outperforming classical gradient descent. Further analysis would thus be interesting.

5. NUMERICAL EXPERIMENTS

We will evaluate the presented methods on a dynamical system with multiplicative noise as in (1) and modes

$$A_1 = \begin{bmatrix} 0.43 & 0.71 \\ -1.13 & 0.43 \end{bmatrix}, B_1 = \begin{bmatrix} 0.36 \\ 0.71 \end{bmatrix}, A_2 = \begin{bmatrix} 0.57 & -0.01 \\ 1.13 & -0.01 \end{bmatrix}, \\ B_2 = 0, A_3 = 0, B_3 = B_1, \text{ and } w_t = (1, v_t),$$

with v_t sampled uniformly from an ellipsoid such that $\mathbb{E}[v_t v_t^\top] = \text{diag}(0.2, 0.5)$. The dynamics were motivated by a control problem of the pitch of a satellite (cf. (Damm, 2003, §1.9.6)), which was discretized using a trapezoid method (Schurz, 1999).

We begin with a setup that works best for PI and compare it to SI. Next we compare PG, PI and SI when data is generated as prescribed by Alg. 2. Afterwards PI is evaluated in an on-policy setting and finally we examine the effect of the tuning parameter β_0 on PI.

5.1 Off-policy PI

First we investigate the effect of the number of rollouts on the performance of our policy iteration scheme. Following the notation of §4.1, take the additive noise radius $r_\nu = 0.1$ and no controller perturbation (i.e. $r_U = 0$). Each policy update uses $M = 30$ trajectories of length $T = 100$ are generated, starting from states distributed with $r_x = 1$.

A fixed, stabilizing control gain $K_0 = [0.5 \text{ } -0.75]$ is used to generate the samples. When data is generated using an unstable controller, PI and PG would fail to converge. Both schemes would also encounter numerical issues. These can be reduced by using more rollouts with a reduced horizon. Further discussion on the effect of stability on PI – specifically due to unstable controllers being generated by the algorithm – is provided at the end of this section.

We initialize PI with

$$\hat{\pi}_0 = (10, 0, -2.8284, 4, 4.2426, 4), \text{ and } \beta_0 = 2000,$$

unless mentioned otherwise. The optimal controller for this initial Q-function equals K_0 and is thus stabilizing. Note that SI requires no initial guess, which can be considered an advantage.

We terminate after 5000 iterations and repeat the whole process 25 times to evaluate variances. Fig. 2 depicts the comparison between SI and PI. For each control gain K and associated π we solve the Lyapunov equation (11) for the true \mathcal{E} to find value function J_π . We then compare $J_\pi(I)$ to the optimal $J_*(I)$ from (4). This is equivalent to comparing the trace of the associated Hessians or the

expected infinite closed-loop horizon cost starting from a random x_0 with $\mathbb{E}[x_0 x_0^\top] = I$. The top plots depict the relative error. The bottom plots show $\|K - K_*\|_2 / \|K_*\|_2$, i.e. the relative spectral norm error with the optimal gain.

Observe how the suboptimality acts like $1/N$ with N the number of samples, while the controller error acts like $1/\sqrt{N}$ for both PI and SI (the dashed lines follow these rates exactly). This corresponds to the rates predicted in (Coppens and Patrinos, 2022, Thm. VI.4).

For future experiments we will depict the suboptimality only. The control error – which decreases at $1/\sqrt{N}$ for all experiments whenever the suboptimality decreases at $1/N$ – is omitted hereafter.

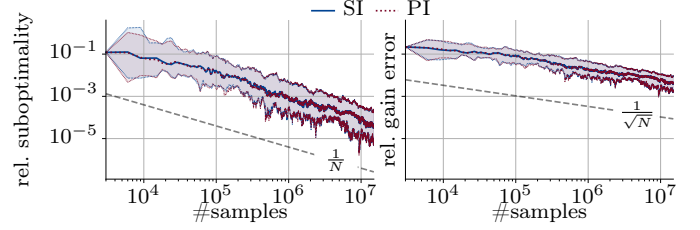


Figure 2. Suboptimality and controller error for off-policy SI and PI with additive exploration noise and $M = 30$. The colored area depicts a 80% two-sided empirical confidence interval.

5.2 Evaluation of PG

Next we consider natural PG. We tune the data-generation such that PG performs well and then pass the data to SI and PI to compare. Here $r_\nu = 0$ and $r_U = 0.15$ produced good results for PG. As before we take $M = 3000$ and $T = 100$. We initialize PG with $K_0 = [0.5 \text{ } -0.75]$ and use the PG gain in later iterations as described in Alg. 2. The step size is set to $7.5 \cdot 10^{-3}$. We initialize PI with $\beta_0 = 5.0$. This change compensates for the absence of additive noise, which makes the data less informative. It corresponds to more trust in the initial guess to avoid generating unstable controllers, which causes PI to diverge. Another experiment below expands on this intuition. We continue for 250 iterations. The rest of the procedure is identical to before and the result is depicted in Fig. 3.

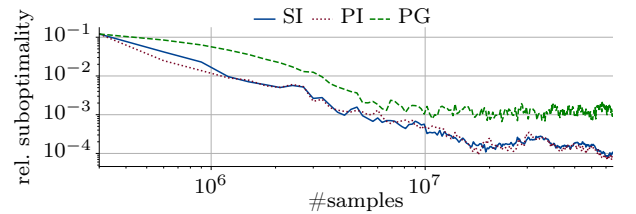


Figure 3. Median relative suboptimality SI, PI and PG.

Note how SI and PI act similarly to before, while PG stagnates after a certain number of iterations. This is also predicted by the theory in Gravel et al. (2021). We can evaluate the sample complexity by repeating the same experiment, but with $M = 300, 3000$ and 30000 . We plot the number of iterations on the horizontal axis to ease visual comparison, keeping in mind that the number of

samples observed per iteration differs. The result in Fig. 4 indicates that the suboptimality improves with $1/M$. So overall the rate is the same as SI and PI, but it manifests in terms of the number of rollouts per gradient evaluation, instead of the cumulative sample count. Moreover, while SI and PI put no requirements on data generation, PG is more restrictive.

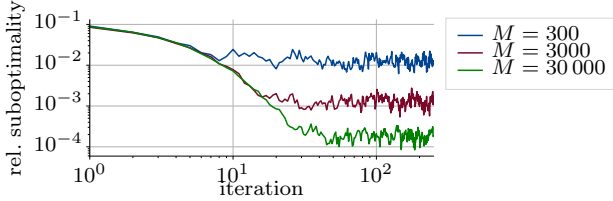


Figure 4. Evaluation of sample complexity of PG. Plots show median relative suboptimality.

5.3 On-policy PI

We can run PI in an on-policy setting with one rollout each iteration. Taking $T = 100$, $M = 1$ and x_0 distributed with $r_x = 1$, while using the final state of the latest iteration afterwards (c.f. continuous mode in §4.1). We initialize PI with $\beta_0 = 100$ and run the scheme for 1000 iterations. The rest of the setup is identical to the first experiment, but now instead of applying K_0 for every iteration, the latest PI control gain is used instead. The result, manifesting the same sample complexity as before, is depicted in Fig. 5. Interestingly the suboptimality is reduced compared to Fig. 2, potentially indicating that this method of data-generation is more informative.

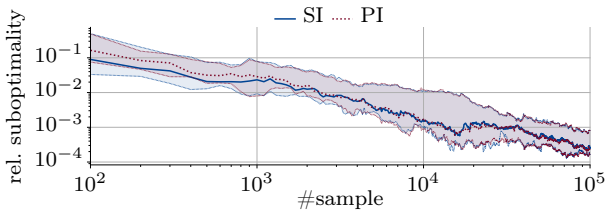


Figure 5. On-Policy PI and SI. The colored area depicts a 80% two-sided empirical confidence interval.

5.4 Tuning of PI

When a small number of samples are provided per iteration in PI, unstable control gains can be generated. This can cause the algorithm to diverge.⁴ To examine the effect of tuning we set $T = 10$ and $M = 5$ and run the algorithm 1000 times for 100 iterations. The remainder of the setup is the same as the first experiment of this section. The data-generation uses the same stabilizing policy $K_0 = [0.5 \text{ } 0.75]$ for each iteration.

The percentage of unstable policies per iteration is depicted in Fig. 6. Note how unstable policies are produced in the first iterations due to the small amount of data and mostly remain unstable afterwards. Low values for

β_0 reduces the number of unstable policies since the algorithm trusts the initial guess more. For $\beta_0 = 0.1$ no unstable policies occur. Alternatively, performing system identification separately from control synthesis does not encounter stability issues and requires no tuning.

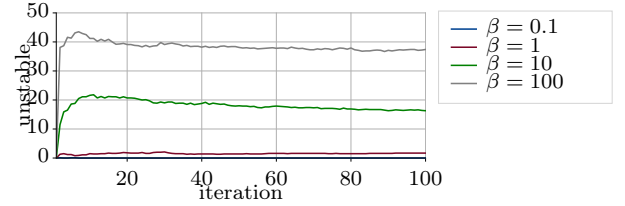


Figure 6. Percentage of unstable policies produced by PI for different tunings.

6. CONCLUSION

From the experiments in the previous section one can conclude a pay-off between a simple implementation and robustness. The policy gradient scheme requires the most effort to tune and requires the most specific data, yet is simple to implement. Meanwhile the model-based approach requires solving a large least-squares problem and a generalized algebraic Riccati equation – usually formulated as a SDP. However it requires no tuning and can handle almost all data-generation schemes. The presented policy iteration scheme meanwhile also solves a smaller least-squares problem, yet avoids the Riccati equation. However as shown in Fig. 6, with limited data the scheme can require some tuning to work.

In future work we will investigate adaptive iteration lengths to avoid such tuning issues. After all, problems often occur in the first iterations. Hence gathering more data there would aid in stabilizing the algorithm. The connection with EKF in §A will also be exploited further to find stability and convergence guarantees. Such a theoretical analysis would also aid in improving tuning.

ACKNOWLEDGEMENTS

We thank Jean-Louis Carron for performing an initial comparison of learning control schemes for multiplicative noise during their master thesis, motivating the developments presented here.

REFERENCES

- Bertsekas, D.P. (2012). *Dynamic Programming and Optimal Control – Vol II*. Athena scientific, 4th edition.
- Bertsekas, D.P. (2016). *Nonlinear programming*. Athena scientific, 3rd edition.
- Bertsekas, D.P. (2022a). *Abstract Dynamic Programming*. Athena scientific, 3rd edition.
- Bertsekas, D.P. (2022b). Newton’s method for reinforcement learning and model predictive control. *Results in Control and Optimization*, 7, 100–121.
- Bradtke, S., Ydstie, B., and Barto, A. (1994). Adaptive linear quadratic control using policy iteration. In *ACC*, volume 3, 3475–3479. IEEE.
- Bradtke, S.J. (1996). Linear least-squares algorithms for temporal difference learning. *Machine Learning*, 22, 33–57.

⁴ See (Bertsekas, 2022a, §3), which proves convergence of PI over the class of stable policies and illustrates what happens when an unstable policy is used instead.

Bu, J., Mesbahi, A., Fazel, M., and Mesbahi, M. (2019). LQR through the Lens of First Order Methods: Discrete-time Case. arXiv: 1907.08921.

Coppens, P. and Patrinos, P. (2020). Sample Complexity of Data-Driven Stochastic LQR with Multiplicative Uncertainty. In *CDC*, 6210–6215. IEEE.

Coppens, P. and Patrinos, P. (2022). Safe learning LQR of linear dynamics with multiplicative noise. arXiv: 2207.06062.

Coppens, P., Schuurmans, M., and Patrinos, P. (2020). Data-driven distributionally robust LQR with multiplicative noise. In *L4DC*, volume 120, 521–530. PMLR.

Damm, T. (2003). Stability of linear systems and positive semigroups of symmetric matrices. In *Positive Systems*, 207–214. Springer.

Damm, T. (2004). *Rational Matrix Equations in Stochastic Control*. Lecture Notes in Control and Information Sciences. Springer, 1st edition.

Dean, S., Mania, H., Matni, N., Recht, B., and Tu, S. (2019). On the Sample Complexity of the Linear Quadratic Regulator. *Foundations of Computational Mathematics*, 1–43.

Gravell, B., Esfahani, P.M., and Summers, T. (2020). Robust control design for linear systems via multiplicative noise. *IFAC-PapersOnLine*, 53(2), 7392–7399.

Gravell, B., Esfahani, P.M., and Summers, T. (2021). Learning optimal controllers for linear systems with multiplicative noise via policy gradient. *TAC*, 66(11), 5283–5298.

Gravell, B., Gargiani, M., Lygeros, J., and Summers, T.H. (2022). Policy Iteration for Multiplicative Noise Output Feedback Control. arXiv: 2203.17165.

Lewis, F.L. and Vrabie, D. (2009). Reinforcement learning and adaptive dynamic programming for feedback control. *IEEE Circuits and Systems Magazine*, 9(3), 32–50.

Mania, H., Tu, S., and Recht, B. (2019). Certainty equivalence is efficient for linear quadratic control. In *NeurIPS*, volume 32.

Mohler, R., Bruni, C., and Gandolfi, A. (1980). A systems approach to immunology. *Proceedings of the IEEE*, 68(8), 964–990.

Recht, B. (2019). A Tour of Reinforcement Learning: The View from Continuous Control. *Annual Review of Control, Robotics, and Autonomous Systems*, 2(1), 253–279.

Schurz, H. (1999). The Invariance of Asymptotic Laws of Linear Stochastic Systems under Discretization. *ZAMM-Journal of Applied Mathematics and Mechanics*, 79(6), 375–382.

Silver, D., Schrittwieser, J., Simonyan, K., Antonoglou, I., Huang, A., Guez, A., Hubert, T., Baker, L., Lai, M., Bolton, A., Chen, Y., Lillicrap, T., Hui, F., Sifre, L., Van Den Driessche, G., Graepel, T., and Hassabis, D. (2017). Mastering the game of Go without human knowledge. *Nature*, 550(7676), 354–359.

Todorov, E. (2005). Stochastic Optimal Control and Estimation Methods Adapted to the Noise Characteristics of the Sensorimotor System. *Neural Computation*, 17(5), 1084–1108.

Wang, F. and Balakrishnan, V. (2002). Robust Kalman filters for linear time-varying systems with stochastic parametric uncertainties. *IEEE Trans. Signal Process.*, 50(4), 803–813.

Wang, T., Zhang, H., and Luo, Y. (2018). Stochastic linear quadratic optimal control for model-free discrete-time systems based on Q-learning algorithm. *Neurocomputing*, 312, 1–8.

Wonham, W.M. (1967). Optimal Stationary Control of a Linear System with State-Dependent Noise. *SIAM Journal on Control*, 5(3), 486–500.

Xing, Y., Gravell, B., He, X., Johansson, K.H., and Summers, T. (2021). Identification of Linear Systems with Multiplicative Noise from Multiple Trajectory Data. 1–50, arXiv: 2106.16078.

Young, P.C. (2011). *Recursive Estimation and Time-Series Analysis*. Springer, 2nd edition.

Appendix A. EKF INTERPRETATION

Introduction to Extended Kalman Filters: Classically an EKF is applied to a nonlinear least-squares problem:

$$\underset{\theta}{\text{minimize}} \quad \frac{1}{2} \|g(\theta)\|_2^2 = \frac{1}{2} \sum_{i=1}^N \|f_i(\theta)\|_2^2.$$

It linearizes $f_i(\theta)$ around recursive estimates of the minimizer θ_k , denoted as $\tilde{f}_i(\theta|\theta_k) := f_i(\theta_k) + \nabla f_i(\theta_k)^\top (\theta - \theta_k)$. These estimates are then computed recursively as (Bertsekas, 2012, Eq. 2.129):

$$\theta_k \in \underset{\theta}{\text{argmin}} \sum_{\ell=1}^k \|\tilde{f}_\ell(\theta | \theta_{\ell-1})\|_2^2, \quad k = 1, \dots, N. \quad (\text{A.1})$$

Our scheme applies the same idea instead to a projected equation of the form

$$\hat{\theta} \in \underset{\theta}{\text{argmin}} \sum_{i=1}^M \|\varphi_i^\top \theta - h_i(\hat{\theta})\|_2^2, \quad (\text{A.2})$$

where we now linearize h_i at each step, producing an algorithm like

$$\hat{\theta}_k \in \underset{\theta}{\text{argmin}} \sum_{\ell=1}^k \|\varphi_i^\top \theta - \tilde{h}_i(\hat{\theta}_k | \theta_{\ell-1})\|_2^2. \quad (\text{A.3})$$

Instead of linearizing each time step however we split the data up into batches and linearize at the start of each batch. Next, this reasoning is applied to our setting.

EKF Policy Iteration: We reinterpret Alg. 1 as an *Extended Kalman Filter* applied to a projected Bellman equation. Following the notation of §3.1, a policy update looks like:

$$\pi_+ = \underset{\pi'}{\text{argmin}} \mathcal{F}_{\pi'} \mathcal{Q}_\pi, \text{ with } \mathcal{Q}_\pi = \mathcal{F}_\pi \mathcal{Q}_\pi.$$

Note that \mathcal{F}_{π_+} is linear in \mathcal{Q} and $\mathcal{F}_{\pi_+} \mathcal{Q}_\pi = \mathcal{F} \mathcal{Q}_\pi$. Thus

$$\mathcal{F} \mathcal{Q}_\pi + \mathcal{F}_{\pi_+} (\mathcal{Q} - \mathcal{Q}_\pi) = \mathcal{F}_{\pi_+} \mathcal{Q} \geq \mathcal{F} \mathcal{Q}, \quad \forall \mathcal{Q}.$$

So \mathcal{F}_{π_+} acts as a supergradient of \mathcal{F} and $\mathcal{F}_{\pi_+}(\mathcal{Q})$ is a linearization of $\mathcal{F}(\mathcal{Q})$ at \mathcal{Q}_π .

Similar to §4.1 we consider a linear parametrization of \mathcal{Q}

$$\mathcal{Q}^\theta(Z) := \text{vec}_s^\top(Z) \theta$$

and introduce the sampled Bellman operator:

$$(\mathcal{F}_\pi^i \mathcal{Q})(Z) = \text{Tr}[ZH] + \mathcal{Q}(\pi(\mathcal{E}_i(Z))).$$

and let $\mathcal{F}^i \mathcal{Q} = \min_\pi \mathcal{F}_\pi^i \mathcal{Q}$.

Consider now the projected Bellman equation⁵ (Bertsekas, 2012, §6.3):

$$\hat{\theta}_\pi = \underset{\theta}{\text{argmin}} \sum_{i=1}^N \|\mathcal{Q}^\theta(Z_i) - (\mathcal{F}^i \mathcal{Q}^{\hat{\theta}_\pi})(Z_i)\|_2^2. \quad (\text{A.4})$$

This is our specific case of (A.2). We can view Alg. 1 as solving (A.4) through a scheme reminiscent of an EKF. Specifically we split the data into batches of size N_k denoted as $\mathcal{I}_k = (\bar{N}_{k-1} + 1, \bar{N}_{k-1} + 2, \dots, \bar{N}_{k-1} + N_k)$, with $\bar{N}_k = \sum_{\ell=1}^k N_\ell$ and $\bar{N}_0 = 0$.

The algorithm then updates $\hat{\theta}_{\pi_k}$ each iteration as (cf. (A.3)):

$$\hat{\theta}_{\pi_k} = \underset{\theta}{\text{argmin}} \left\{ \sum_{\ell=1}^k \sum_{i \in \mathcal{I}_\ell} \|\mathcal{Q}^\theta(Z_i) - (\mathcal{F}_{\pi_\ell}^i \mathcal{Q}^{\hat{\theta}_{\pi_k}})(Z_i)\|_2^2 \right\},$$

where we linearized the term in the norm of (A.4) by taking π_ℓ such that $\mathcal{F} \mathcal{Q}^{\hat{\theta}_{\pi_{\ell-1}}} = \mathcal{F}_{\pi_\ell} \mathcal{Q}^{\hat{\theta}_{\pi_{\ell-1}}}$. Unlike in classical

⁵ Here $\mathcal{Q}^{\hat{\theta}_\pi}$ is the parametrized \mathcal{Q}_π .

EKF we linearize only at the start of each batch, not for each sample. This aids in stabilizing the algorithm.

To make the connection with Alg. 1 complete we re-introduce the notation of §3.2. Specifically $b_i = \text{Tr}[HZ_i]$, $g_i = \text{vec}_s(Z_i)$, $g_{i+} = \text{vec}_s(\pi_{\ell-1}(X_{i+1}))$ and $a_i = g_i - g_{i+}$. Then we get:

$$\hat{\theta}_{\pi_k} = \underset{\theta}{\text{argmin}} \left\{ \sum_{i=1}^{\bar{N}_k} \|g_i^\top \theta - g_{i+}^\top \hat{\theta}_{\pi_k} - b_i\|_2^2 \right\}, \quad (\text{A.5})$$

which is equivalent to the following normal equations:

$$\sum_{i=1}^{\bar{N}_k} g_i((g_i^\top - g_{i+}^\top)\hat{\theta}_{\pi_k} - b_i) = \sum_{i=1}^{\bar{N}_k} g_i(a_i^\top \hat{\theta}_{\pi_k} - b_i) = 0.$$

This corresponds to the normal equation of least-squares with IVs, hence motivating their use in §3.2. We can use the recursion (17) to generate solutions iteratively without computing inverses.

Specifically we add a regularization term

$$\|\theta - \hat{\theta}_{\pi_0}\|_{S_{\pi_0}^{-1}}^2/2$$

to (A.5). The updates can then be computed recursively by solving a one-stage normal equation each time:

$$g_i(a_i^\top \hat{\theta}_{\pi_k} - b_i) + S_{\pi_k, i-1}^{-1}(\hat{\theta}_{\pi_k} - \hat{\theta}_{\pi_k, i-1}) = 0. \quad (\text{A.6})$$

The solution of which is

$$\hat{\theta}_{\pi_k, i} = (S_{\pi_k, i-1}^{-1} + g_i a_i^\top)^{-1} (S_{\pi_k, i-1}^{-1} \hat{\theta}_{\pi_k, i-1} + g_i b_i). \quad (\text{A.7})$$

The first factor is simplified through Woodbury's matrix identity applied to the first factor and introducing $L_i = S_{\pi_k, i-1} g_i / (1 + a_i^\top S_{\pi_k, i-1} g_i)$ to

$$\begin{aligned} S_{\pi_k, i} &:= (S_{\pi_k, i-1}^{-1} + g_i a_i^\top)^{-1} \\ &= S_{\pi_k, i-1} - (L_i a_i^\top) S_{\pi_k, i-1}. \end{aligned} \quad (\text{A.8})$$

Plugging into (A.7) gives

$$\hat{\theta}_{\pi_k, i} = \hat{\theta}_{\pi_k, i-1} + L_i [b_i - a_i^\top \hat{\theta}_{\pi_k, i-1}].$$

Also, by combining this with (A.7) and (A.8) we can show that (A.6) is equivalent to

$$S_{\pi_k, i}^{-1}(\hat{\theta}_{\pi_k} - \hat{\theta}_{\pi_k, i}) = 0. \quad (\text{A.9})$$

So we can equivalently process the next terms in (A.5) by adding the left-hand side of (A.9) as a regularization term. As such we have derived the recursion in (17).